Mechanical Characterization of Gold Nanowires

Ming Chang[1, 2, #], Xiaojun Liu[2], Feng-Cheng Chang[1], Juti R Deka[3] and Hong-Wen Wang[3]

1 Department of Mechanical Engineering, Chung Yuan Christian University, Chung Li, Taiwan 32023
2 School of Mechanical Science & Engineering, Huazhong University of Science & Technology, Wuhan, Hubei, China 430074
3 Department of Chemistry, Chung Yuan Christian University, Chung Li, Taiwan 32023
Corresponding Author / E-mail: ming@cycu.edu.tw, TEL: +886-3-265-4303, FAX: +886-3-265-4399

KEYWORDS : Mechanical Characterization, Gold Nanowire, Nanomanipulator, Tensile Test, Bucking Test, Bending Test

Mechanical properties of gold nanowires were determined in this investigation using a multifunctional nanomanipulator inside a scanning electron microscope (SEM). Gold nanowires were synthesized by electrochemical deposition (ECD) technique. Three different characterization techniques including tensile, buckling and bending tests had been adapted to quantitatively determine Young's modulus, yield stress and fracture stress of the gold nanowires. The mechanical characterizations show that the nanowires were highly flexible in nature. The excellent resilience and the ability to store elastic energy in these nanowires confirm their potential applications in nano electromechanical devices.

Manuscript received: January XX, 2011 / Accepted: January XX, 2011

1. Introduction

Nanowires (NWs) have a wide range of potential applications in opto-electronic nanodevices [1], biological sensors [2], and nanoelectronic circuits [3]. As NWs have large surface to volume ratio as compared to bulk materials, considerable research interest has been developed in the measurement of the material properties of NWs. Metallic NWs have extensive applications as interconnecting leads and functional building blocks in nanodevices and nanoelectronics because of their unique electrical and mechanical properties [4]. Amongst metallic NWs gold NW is getting more attention in nanotechnology due to their capacity for biomolecule functionalization [5, 6], high conductivity [7] and distinct optical properties [8]. Due to these extraordinary behaviors, great efforts have been made to synthesize gold NW with different techniques.

Although gold NWs are touted as the next generation material for use in nanoscale systems, its mechanical properties are still not well explored [9]. It is significant and essential to study accurately and reliably the mechanical characteristics of individual gold NW for fundamental understanding of deformation behavior at the nanoscale which is important for development and processing of novel nanowire-based devices. Mechanical characterization of individual NW is challenging due to its extremely small dimension, difficulty in manipulation, alignment and gripping, and requirement of application and measurement of very high resolution force and displacement [10].

This investigation reports on the measurement of mechanical properties of individual electrochemically grown gold NWs inside an SEM using a custom made nanomanipulator. The ends of the NWs were clamped between two AFM tips attached with the nanomanipulator stages for in situ mechanical characterizations. The NWs for this work were prepared by using electrochemical deposition (ECD) method [11, 12]. Three different techniques including tensile, buckling and bending tests had been performed for mechanical characterizations of the NWs. The mechanical characterizations reveal high flexibility of the gold NWs.

2. Synthesis of Gold Nanowire and its Morphological and Microstructural Study

Gold NWs were grown inside commercial polycarbonate (PC) membrane templates (300 nm pore channel size) using ECD method [13]. Gold solution of 0.1 wt% for the ECD was prepared by dissolving 1gm gold foil in 10 ml aqua regia diluted in 100 ml de-ionized water and subsequently heated at 90 °C for 30 min. To ensure good electrical contact during the deposition, the back of the PC membrane template was sputter coated with gold before being attached to the working electrode which was a stainless steel sheet of 9 mm diameter. This working electrode was placed underneath the template and a platinum mesh was used as the counter electrode. The distance between the two electrodes was kept as 30 mm. Gold NWs were deposited by applying 1V for 3h. The sample with the working electrode was immersed in CH_2Cl_2 solution for 30 min to dissolve the PC membrane. The deposited NWs were remained on the flat working electrode and stuck to the surface on drying.

Scanning electron microscope (SEM, Hitachi 4100) and transmission electron microscope (TEM, JEOL 2010) were used to study the morphology and microstructure of the prepared gold NWs. The samples were ultrasonically dispersed in alcohol to form nano-

material suspension and dropped onto carbon film supported with a metal holder for TEM study.

SEM image shown in Fig. 1(a) indicates that plenty of gold NWs were formed on electrochemical deposition of gold on PC membrane. The formed NWs were quite clean with no contamination attached to their surfaces. The lengths of gold NWs were measured to be 5-20 μm. Some of the NWs were observed to be aggregated into bundles and looked wider than others in the SEM image. TEM image of the gold NW is shown in Fig. 1(b). Detailed examination of the NW along their length revealed that they were uniform in width; smooth surface and free of defects. The NWs were of high purity and homogenous in nature. The study of the cross-sectional morphology of the NW specified that the NWs had circular cross-sections and diameter ranging from 150-350 nm. Figure 2 shows the SEM image of circular cross-section of a NW.

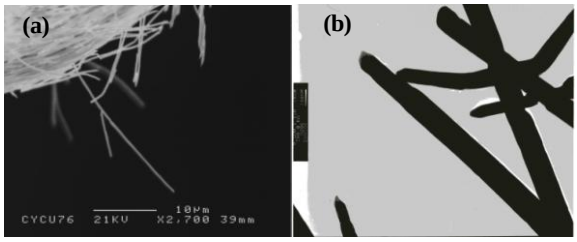

Fig. 1 (a) SEM and (b) TEM images of gold nanowires

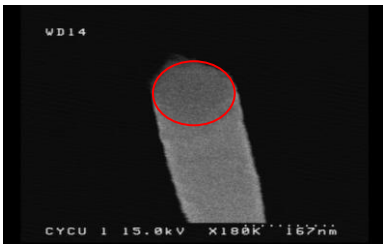

Fig. 2 SEM image showing the cross-section of a nanowire

3. Design and Fabrication of a Nanomanipulator for in-situ Mechanical Characterization

Due to the extremely small size of NW in-situ mechanical characterization is a challenge. In-situ nanomanipulation relies on high magnification SEM images as a visual feedback system in order to interact with a nanoscale target using a probe, which has been extensively utilized to characterize the mechanical and electrical properties of novel nanostructures [14]. Well-controlled lateral and longitudinal motions are necessary for manipulation of nanostructures. A nanomanipulation system was developed using commercially available actuators and positioning stages to use inside limited space within an SEM for in-situ mechanical characterizations. The positioning stages of the manipulator were equipped with AFM tips for both manipulation of NWs and measurements.

As shown in Fig. 3, the nanomanipulator was designed by superposition of three linear stages, X, Y, and Z, and one rotational stage (θ) that can move to different ranges and precession. These were referred as coarse and fine movements respectively. The coarse movements along the X, Y and Z axes were based on a parallel-guiding plate-spring mechanism and chosen because of their parallel and precise displacements. This ensured high flexibility and easy re-configurability to the manipulator. The parallel plates were driven by vacuum compatible picomotors (New Focus, 8321-V). The maximum travelling range of the picomotor was 10.0 mm with dynamic step size 30 nm when the picomotor drives at 2 KHz. The rotational stage movement was achieved by mounting a rotating picomotor on the top of the Z-stage which can provide angular step sizes less than 0.02°.

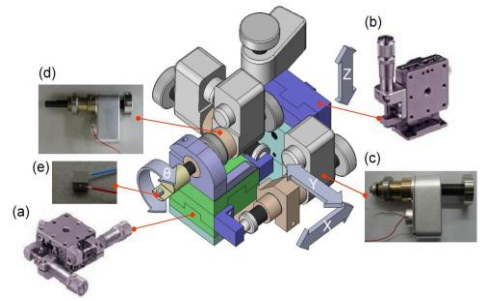

Fig. 3 Schematic of the nanomanipulator

The fabricated nanomanipulator was placed inside a JEOL-JSM6300 SEM to perform manipulation, electrical and mechanical characterizations of gold NWs. The maximum resolution of the SEM is 3.5 nm at 30 kV. The X-Y stage of the manipulator guided motion parallel to the x-y plane of SEM stage and the Z stage was used for the motion along the SEM beam axis. Two AFM tips of known spring constants FPC10, AIST (~0.066Nm^{-1}) and BS-Tap300Al (~40Nm^{-1}) were fixed to the rotating picomotor and X-Y stage respectively, to hold a NW for mechanical characterization. Rigid tip was used to manipulate the NW from the source and whereas the soft tip served as a load sensor. Independent three axes relative displacements between tip and sample can be achieved with this customized design. The details about the design and fabrication of the nanomanipulator are given elsewhere [15, 16].

4. Manipulation and Mechanical Characterization of a Nanowire with the Nanomanipulator

Picking of single NW from its source and clamping it along the axis of load application was a difficult task in performing mechanical characterization. The rigid cantilevered tip was first mechanically fixed to the rotating picomotor and used for manipulation of a NW from its source placed on the X-Y stage of the nanomanipulator. This tip was brought into mechanical contact with the top of a NW by supplying necessary voltage to the attached picomotor. Due to Van der Waals force, the NW end stuck to the tip. Amorphous carbon was deposited at the tip-nanowire junction to make the contact more rigid [17]. A deposit at least 100 nm square was typically made at each nanowire-tip junction and was usually a strong enough attachment to allow the loading and breaking of NW before attachment failed. The NW was picked up from the source by applying enough force to the cantilever. The tip along with the NW was then detached from the Z-stage and fixed to the X-Y stage. The free end of the NW was clamped to the soft cantilevered tip which was fixed on the Z-stage.

4.1 Evaluation of Mechanical Properties with Tensile Test

Tensile test, a quasi-static test is generally used for mechanical characterization of nanotubes, nanowires and nanofibers of short lengths. A continuously increasing load P was applied to the NW end fixed to the rigid cantilever to elongate the NW until it fractured. The stress distribution on the cross section of a NW due to the axial load

during the test depends upon the way how the axial load is actually applied. A schematic diagram of the tensile test is given in Fig. 4. The loading process was recorded in a series of SEM images to estimate the applied load and corresponding change in distance between the AFM tips. As it must be relied on image analysis to measure the load and displacement, proper specimen alignment was a critical task. This was accomplished very carefully adjusting the tips position until both were in focus before final clamping. The entire NW was kept in the SEM image to accurately determine the length of the NW. Figure 5 shows the SEM images of elongation of a NW due to applied load. The images show that the deflection of the soft cantilever increases as the rigid cantilever is moved in the downward direction. The NW finally broke into two parts. The soft cantilever returned back to original position after the NW was broken. The SEM image of a NW captured after breaking is presented in Fig. 6. As shown, the NW of original length 8 μm was stretched and broken in the middle.

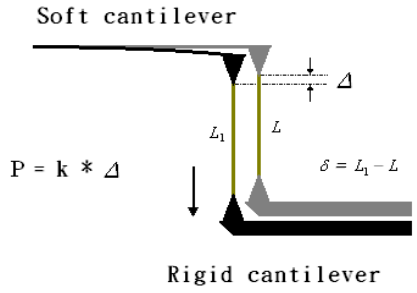

Fig. 4 Schematic diagram of tensile tests

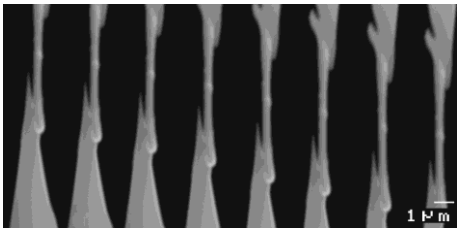

Fig. 5 SEM images of tensile test on a gold nanowire

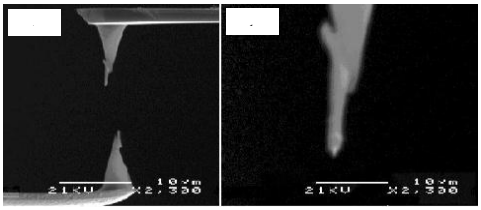

Fig. 6 (a) SEM image of breaking of a nanowire; (b) A part of the broken nanowire

The deflection d of the soft cantilever at each loading and the length of the NW were estimated from the pixel resolution of the images. The maximum deflection of the cantilever was measured to be less than 5% of its length and therefore the applied load P was determined as P = d × k [18] where 'k' is the spring constant of the soft cantilever and 'd' is the cantilever deflection. The axial deflection (elongation) δ of the NW due to application of load P was determined from the change in length of NW in the recorded images. With the knowledge of the linear elasticity, Young's modulus of NWs were determined using Hooke's law as

$$E = \frac{P L}{\delta A} = \frac{\sigma}{\varepsilon} \quad (1)$$

where A is the area of cross section of the NW, L is the original length of the NW, σ and ε are the axial stress and strain of the NW in the linear elasticity range, respectively. The stress-strain plot of a gold NW of length 8 μm and diameter 150 nm is shown in Fig. 7. The Young's modulus, yield stress and fracture stress of the NW can be determined from this stress-strain diagram as 21.6 GPa, 151 MPa and 241 Mpa, respectively. Several nanowires were tested and the measured mechanical characteristics of four different NWs are shown in Table 1. The average Young's modulus is roughly 20 ± 2 GPa and the yield and fracture stresses are dependent on the section area. As it is shown, NWs with bigger section area got bigger strength. In some cases the NW being tested was not perfectly aligned with the axis of the applied load as SEM provides only top view of the NW. As a result it can measure misalignment in the x-y plane but cannot detect slight height mismatch in the z-direction. The method developed by Ding et. al [19] for the determination of effect of in-plane misalignment and height mismatch on the load and strain during the tensile testing was used to minimize the error in measurement.

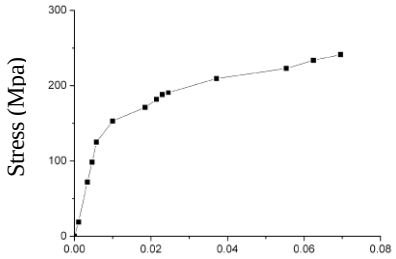

Fig. 7 Stress-strain diagram of a gold nanowire under tensile load

NW	Length (μm)	Radius (μm)	Young's modulus (GPa)	Yield Stress (MPa)	Fracture Stress (MPa)	Fracture Strain (%)
1	6.821	0.137	21.4	125	222	17.3
2	8.022	0.150	21.6	151	241	7.2
3	6.272	0.102	18.3	113	165	14.3
4	6.452	0.121	19.7	122	192	12.1

Table 1 Young's modulus of nanowire with tensile test

4.2 Buckling Test

Two different modes for structure collapse, yielding and buckling are generally observed in compression test. Yielding mode dominates the structure collapse for the short column and it changes to buckling mode due to the instability of structure at the large length to diameter ratio. For the given length smaller diameter column undergo Euler type buckling, whereas for larger diameter buckling is not observed. As the column buckles, instead of remaining straight, it becomes sharply curved. Young's modulus is then measured from the buckling mode of the column due to application of axial compressive load.

In the compression test, axial loads were continuously applied to the NW by moving the X-Y stage of the manipulator in upward direction using the picomotor attached to the stage. The load deflected the soft cantilever which was connected to the rigid cantilever through the NW. It was made sure that the NW buckled perpendicular to the direction of the electron beam to reduce the probability of any hidden displacement along the electron beam direction which may alter the actual measurement results. On application of certain load i.e.

the critical load P_{cr}, NW transformed to buckling mode along the principal axis of cross-section having least moment of inertia as [15],

$$P_{cr} = \frac{\pi^2 EI}{(KL)^2} \quad (2)$$

where $I = (\pi r^4/4)$ is the moment of inertia and KL is the effective length of the NW. As one end of the NW was fixed to rigid cantilever and the other to soft cantilever, it can be assumed as fix-pin model for which K = 0.7. The end condition constant can be also determined from the distance between two adjacent inflection points of the buckling shape. Equation (2) indicates that the critical load for buckling instability development is proportional to $1/L^2$ and I. Figure 8 shows a series the SEM images of change of modes of the NW with the application of axial load. The change in shape can be summarized as, when (i) $P < P_{cr,}$ the NW is in stable equilibrium and bent slightly; (ii) $P = P_{cr}$, NW is in neutral equilibrium and bent amplitude could be arbitrary; and (iii) $P>P_{cr}$, NW is on unstable equilibrium and buckled laterally under the slightest disturbance. The corresponding applied force with respect to lateral deflection of a gold NW of length 14.40 μm and diameter 338 nm is shown in Fig. 9. The critical load (P_{cr}) was determined to be 1.378 μN from the force-deflection curve which indicates high flexibility of the NW. Young's modulus of several NWs of different lengths and cross sections were determined and estimated to be roughly 22 ± 2 GPa, as shown in Table 2. Bigger Young's modulus can be found at NWs with smaller length to diameter ratio.

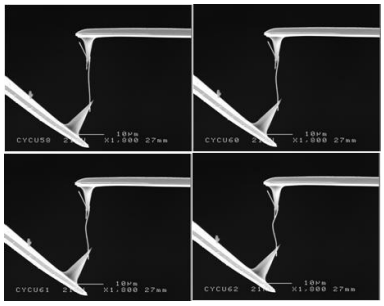

Fig. 8 Series of SEM image of buckling of a gold nanowire

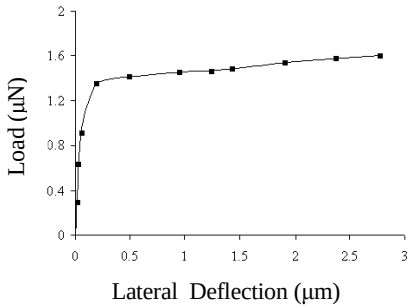

Fig. 9 Load-deflection curve of a gold nanowire due to buckling

NW	Length (μm)	Radius (μm)	Buckling Force (μN)	Moment of inertia $\times 10^{-3}$ (μm^4)	Young's modulus (GPa)	Length / diameter
1	15.041	0.172	1.473	0.172	24.08	43.7
2	14.404	0.169	1.378	0.641	22.14	42.61
3	19.058	0.152	0.479	0.419	20.61	62.69
4	15.880	0.152	0.731	0.419	21.84	52.23

Table 2 Young's modulus of nanowires with buckling test

4.3 Bending Test

The cantilevered tip containing the NW was mounted on the X-Y stage for bending test in such a way that the horizontal axis of the tip became parallel to the longitudinal axis (length) of the NW. The other (free) end of the NW was simply contacted to the soft tip, attached to the rotating picomotor on the Z-stage to perform bend test. In the in-situ bend test, transverse load was applied on individual gold NW by moving the stage containing the rigid cantilever vertically upward after ensuring the alignment of the ends of the NW. Young's modulus of the NW was measured from the deflection δ at the free end of the NW due to the applied load. The effect of shear was neglected in the determination of load and assumed that the load applied along the central axis of the NW. P and δ were determined from a series of SEM images captured during the test. A sequence of recorded SEM images of bending of a NW is shown in Fig. 10. As the NW gradually bent with the applied force, the vertical separation between the two AFM tips was considered as the deflection of the NW. P was determined from the displacement of the soft cantilever and its spring constant, similar to the compression test and tensile test. Young's modulus was determined from the load-deflection relationship,

$$E = \frac{PL^3}{3I\delta} \quad (3)$$

where L and δ can be determined from the horizontal and vertical distances between the two tips, respectively, in case the NW is horizontally placed prior to force applied. The P-δ curve of a gold NW subjected to bend test is shown in Fig. 11. The plot shows that the mechanical behavior of the NW at the large deflection region was almost same as in the small deflection region. No permanent deformations of the NWs were observed during the test and back to its original position on the removal of the load. The average Young's modulus from bend tests of several dufferent NWs were determined to be roughly 22.5 ± 3 GPa as shown in Table 3.

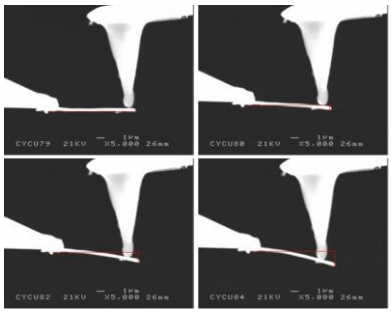

Fig. 10 SEM images of bending of a gold nanowire

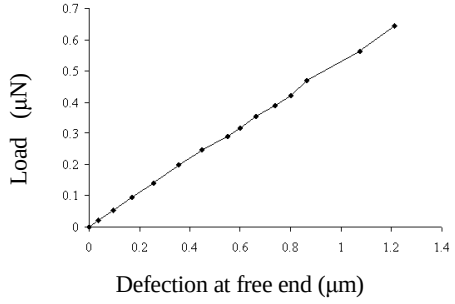

Fig. 11 Load-deflection curve of a gold nanowire caused by bending

NW	Length (μm)	Radius (μm)	Applied load (μN)	Deflection (μm)	Moment of inertia $\times 10^{-3}$ (μm^4)	Young's modulus (GPa)
1	4.81	0.171	0.389	0.813	0.671	25.88
2	10.76	0.173	0.045	1.228	0.704	21.69
3	6.76	0.162	0.026	0.211	0.541	24.25
4	5.12	0.144	0.019	0.131	0.338	19.54

Table 3 Young's modulus of nanowires with bending test

5. Results and Discussion

The average Young's modulus of the gold NWs were measured to be 20 ± 2 GPa, 22 ± 2 GPa, and 22.5 ± 3 GPa with tensile, buckling, and bending tests, respectively. Young's modulus is an intrinsic material property and fundamentally related to internal atomic bonding. The measured values were less than that of their counterpart bulk value which is 78 GPa [20]. An important factor in evaluating the mechanical properties of NW is size effect [21]. As grain sizes or structural dimensions decrease, interatomic reorganization near surfaces gain influence over bulk material behavior. Due to change in atomic coordination and electron distribution, free surfaces in material can have different elastic modulus from the bulk [22, 23]. The non-bulk geometry of the NW can primarily be attributed to the influence of variable surface elasticity. Bond length, bond energy and arrangement of atoms also influence the overall elastic behavior of the material. Molecular dynamics simulation illustrates that if the bond energy between neighboring atoms is significant compared with interaction with other atoms, Young's modulus of the NW will be less than the bulk material [23]. Other factors such as different level of vacancies within the NW due to different synthesis conditions and crystal orientation can contribute in the reduction of Young's modulus [24]. Interfaces, interfacial energy, and surface topography also play increasingly important role in the deformation and failure processes of the NW. Length to diameter ratio affects the deflection of the NW which also influences the Young's modulus.

It is also interesting to note that the measured values of Young's modulus by different testing methods have a little difference. This variation may be due to different boundary conditions assumed for estimation of Young's modulus with different techniques [25]. The effect of end condition constraint on the force–deflection curve of the NW still to a large extent is unknown. Young's modulus of the NW determined with the buckling test was determined to be higher than that obtained with the tensile test. This can be attributed to the dissimilar structural variation of the NW at the same strain during the tensile and compressive processes. Nonlinear elastic response of the NW core plays the greatest role in determining the elastic modulus of NWs subjected to axial tensile or compressive loads [26]. This effect stems from the fact that in equilibrium surface stresses give rise to axial compressive strain in the NW core. As NW size decreases, this compressive strain increases in magnitude because of larger surface to volume ratio. The increase or decrease of the Young's modulus of the NW depends on the crystallographic orientation of the lattice. The different Young's modulus with bend test may be due to the involvement of less surface atoms which are easier to stretch than the atoms locked in the crystal lattice. It can be summarized that the different behaviors of Young's modulus with tensile, compressive and bend tests are not experimental error, but can be due to surface effect, atomic rearrangement, dissimilar structural variation etc.

The dispersion of the measured Young's modulus with each technique was due to the lack of measuring accuracy of displacement, length and diameter of the nanowire. As the sample size becomes smaller and smaller any measuring inaccuracy of the size of the NW may have significant effect on the final result. Equations (1)~(3) show that Young's modulus of a NW is functions of its length and load. Measurements of all the parameters required for the calculation of Young's modulus were restricted by the pixel resolution of the image and applied load direction. Perfect alignment was also difficult to achieve for exact determination of loading direction which may result in variation of moment of inertia. Moreover, average value of diameter of the NW was accounted instead of actual value in the calculation of area and moment of inertia. The dispersion of the Young's modulus measured with the bend test was found to be larger than that measured with tensile and compression tests. The induced stress is concentrated at the upper and lower free surfaces of the NWs during the bend test; however, NW subjected to tension or compression has uniform applied stress through the entire cross section. To accurately measure the mechanical properties, the position of applied force should be calibrated very carefully for the precise determination of deflection of the free end and the length of the NW.

The failure strength of the gold NW was measured to be higher than the bulk gold which is typically around 100 MPa. This can be attributed to the reduction in the number of defects in the NW in comparison to bulk material. Since the fracture process is influenced by defect nucleation and propagation, the probability of failure is less in nano-material and therefore has high fracture stress. Due to bond-length contraction of the surface atoms there was relaxation of the surface and which lead to higher fracture strain. The tiny grain size and small lateral dimensions restrict dislocation activity, driving an increase in yield and fracture strength of NWs.

4. Conclusions

Nanomechanical characterizations of gold NWs with three different methods, tensile, buckling and bending tests have been presented. Mechanical and structural aspects are of critical importance in determining the long-term stability of such small structures. Among the characterization techniques used in this study, bending test present the most convenient way to conduct as it only needs to apply a smaller force and monitor only the deflected end rather than the entire NW. The tensile and buckling tests are more challenging since the NW must be clamped at both ends, stretched or compressed uni-axially, and measured its elongation with nanometer resolution. Compared with buckling and bending tests, tensile test is straightforward and reliable, as the stress state in the specimen tends to be uniform. Moreover, tensile test has the full capacity for the measurement of elastic modulus, yield strength, and tensile strength. The buckling test is a way to determine the Young's modulus for a longer NW under compression which is important for mechanical applications in case the material is not isotropic. In addition, the mechanical properties are observed to be also dependent on the

geometrical condition of the NWs irrespective of the experimental technique. Presence of fewer mechanical defects per unit length offers high strength to the NWs. Such properties are essential to the design and reliability of novel nanodevices. The work provides a better understanding of the mechanical property of gold NWs, as well as gives more options to build nanodevices such as, sensors, electronics, and solar cells etc.

.

ACKNOWLEDGEMENT

The authors gratefully acknowledge the support of the National S cience Council of Taiwan under project number 96-2221-E-033-042-MY3.

REFERENCES

1. Lou, J., Tong, L. and Ye Z., "Modeling of Silica Nanowires for Optical Sensing," Opt. Express, Vol. **13**, pp. 2135–2140, 2005.
2. Cui, Y., Wei, Q., Park, H. and Lieber, C. M., "Nanowire Nanosensors for Highly Sensitive and Selective Detection of Biological and Chemical Species," Science, Vol. 293, pp. 1289–1292, 2001.
3. Lieber, C. M., "Nanoscale Science and Technology: Building a Big Future from Small Things," MRS Bull., Vol. **28**, pp. 486–491, 2003.
4. Kashimura, Y., Nakashima, H., Furukawa, K. and Torimitsu, K., "Fabrication of Nano-Gap Electrodes Using Electroplating Technique," Thin Solid Films, Vol. 438, pp. 317–321, 2003.
5. Wagner P., Hegner M., Kernen P., Zaugg F. and Semenza, G., "Covalent Immobilization of Native Biomolecules onto Au(1 1 1) via N-hydroxysuccinimide Ester Functionalized self-assembled Monolayers for Scanning Probe Microscopy," Biophys J, Vol. 70, pp 2052–66. 1996.
6. Rabkeclemmer, C. E., Leavitt, A. J. and Beebe, T. P., "Analysis of Functionalized DNA Absorption on Au (1 1 1) Using Electron Spectroscopy," Langmuir, Vol. 10, pp. 1796–800, 1994.
7. Kim, N. S., Amert, A. K., Woessner, S. M., Decker, S., Kang, S. M. and Han, K. N., "Effect of Metal Powder Packing on the Conductivity of Nanometal Ink," J Nanosci. Nanotechnol., Vol. 7, pp. 3902–3905, 2007.
8. Rauter, H., Matyushin, V., Alguel, Y., Pittner, F. and Schalkhammer, T., "Nanotechnology for Smart Polymer Optical Devices," Macromol. Symp. , Vol. 217, pp. 109–133, 2004.
9. Bin, W., Andreas, H. and John, B., "Mechanical Properties of Ultrahigh-Strength Gold Nanowires," Nature Materials, Vol. 4, pp. 525-529, 2005.
10. Desai, A. V. and Haque, M. A., "Mechanical Properties of ZnO Nanowires", *Sensors Actuators* A, Vol. 134, pp. 169-176, 2007.
11. Shingubara, S., Okino, O., Sayama, Y., Sakaue, H. and Takahagi, T., "Ordered Two-dimesion Nanowire Array Formation using Self-Organized Nanoholes of Anodically Oxidized Aluminum," Jpn. J. Appl. Phys. , Vol. 36, pp. 7791-7795, 1997.
12. Motoyama, M., Fukunaka, Y., Sakka, T., Ogata, Y. H. and Kikuchi, S., "Electrochemical Processing of Cu and Ni Nanowire Arrays," J. Electroanal. Chem. Vol. 584, pp. 84-91, 2005.
13. Lina, C. C., Juoa, T. J., Jie, C. Y., Chioub, C.H., Wang, H. W. and Liu, Y. L., "Enhanced Cyclic Voltammetry Using 1-D Gold Nanorods Synthesized via AAO Template Electrochemical Deposition," Desalination, Vol. 233, pp. 113–119, 2008.
14. Zhou, W. and Wang, Z. L., Scanning Microscopy for Nanotechnology: Techniques and Applications, Springer, New York, pp. 192–224, 2007.
15. Chang, M., Chung, C. C., Deka, J. R., Lin, C. H., and Chung, T. W., "Mechanical Property of Microwave Hydrothermally Synthesized Titanate Nanowires," Nanotechnology, Vol. 19, 025710, 2008.
16. Chang, M., Lin, C. H., Deka, J. R. and Lin, C. P., "Development of a Versatile Nanomanipulation System and Some of its Typical Applications," to be published in J. CSME, 2011.
17. Ding, W., Dikin, D. A., Chen, X., Piner, R. D., Ruoff, R. S., Zussman, E., Wang, X. and Li, X., "Mechanics of Hydrogenated Amorphous Carbon Deposits from Electron-Beam-Induced Deposition of A Paraffin Precursor," J. Appl. Phys., Vol. 98, 014905, 2005.
18. Ruoff, R. S., Qian, D. and Liu, W. K., "Mechanical Properties of Carbon Nanotubes: Theoretical Predictions and Experimental Measurements," Comptes Rendus Physique, Vol. 4, pp. 993-1008, 2003.
19. Ding, W., Calabri, L., Chen, X., Kohlhaas, K. M. and Ruoff, R. S., "Mechanics of Crystalline Boron Nanowires," Composites Science and Technology, Vol. 66, pp. 1112–1124, 2006.
20. Callister, W. D. Jr, Materials Science and Engineering, Wiley, New York, Ch. 6–8, 1994.
21. Miller, R.E. and Shenoy, V.B., "Size-Dependent Elastic Properties of Nanosized Structural Elements," Nanotechnology, Vol. 11, pp. 139–147, 2000.
22. Sun, C. Q., Tay, B. K., Zeng, X. T., Li, S., Chen, T. P., Zhou, J., Bai, H. L. and Jiang, E. Y., "Bond-Order-Bond-Length-Bond-Strength (Bond-OLS) Correlation Mechanism for the Shape-and-Size Dependence of A Nanosolid," Journal of Physics: Condensed Matter, Vol. 14, pp. 7781-95, 2002.
23. Zhou, L. G. and Huang, H., "Are Surfaces Elastically Softer or Stiffer?" Applied Physics Letters, Vol. 84, pp. 1940-42, 2004.
24. Chang, M., Lin, C. H., Deka, J. R., Chang, F. C. and Chung, C. C., "In Situ Mechanical Property Measurement of Titania Nanowires," Journal of Physics D: Applied Physics, Vol. 42, 145105, 2009.
25. Chen, Y. X., Dorgan, B. L., Mcllroy, D. N. and Aston, D. E., "On The Importance of Boundary Conditions on Nanomechanical Bending Behavior and Elastic Modulus Determination of Silver Nanowires," J. Appl. Phys., Vol. 100, 104301, 2006.
26. Liang, H. Y., Upmanyu, M. and Huang, H. C., "Size-Dependent Elasticity of Nanowires: Nonlinear Effects," Phys. Rev. B, Vol. 71, 241403, 2005.